SMALL GTPASES
2022, VOL. 13, NO. 1, 267–281
https://doi.org/10.1080/21541248.2021.2019503

Taylor & Francis
Taylor & Francis Group

RESEARCH PAPER

Deletion of murine *Rhoh* leads to de-repression of *Bcl-6* via decreased KAISO levels and accelerates a malignancy phenotype in a murine model of lymphoma

Hiroto Horiguchi[a,*], Haiming Xu[a,b,*], Beatrice Duvert[a,*], Felicia Ciuculescu [a,b], Qiuming Yao[a], Amit Sinha[c], Meaghan McGuinness[a], Chad Harris[a], Christian Brendel[a,b,d], Anja Troeger[e], Roberto Chiarle[f], and David A. Williams[a,b,d,g]

[a]Division of Hematology/Oncology, Boston Children's Hospital, Harvard Medical School, Boston, MA, USA; [b]Department of Pediatric Oncology, Dana-Farber Cancer Institute, Boston, MA, USA; [c]BasepairTech, New York, NY, USA; [d]Harvard Stem Cell Institute, Harvard University, Boston, MA, USA; [e]Division of Pediatric Hematology, Oncology and Hematopoietic Stem Cell Transplantation, University Hospital Regensburg, Regensburg, Bavaria, Germany; [f]Department of Pathology, Boston Children's Hospital, Harvard Medical School, Boston, MA, USA; [g]Harvard Medical School, Harvard Initiative for RNA Medicine, Boston, MA, USA

ABSTRACT

RHOH/TFF, a member of the RAS GTPase super family, has important functions in lymphopoiesis and proximal T cell receptor signalling and has been implicated in a variety of leukaemias and lymphomas. RHOH was initially identified as a translocation partner with BCL-6 in non-Hodgkin lymphoma (NHL), and aberrant somatic hypermutation (SHM) in the 5′ untranslated region of the RHOH gene has also been detected in Diffuse Large B-Cell Lymphoma (DLBCL). Recent data suggest a correlation between RhoH expression and disease progression in Acute Myeloid Leukaemia (AML). However, the effects of RHOH mutations and translocations on RhoH expression and malignant transformation remain unknown. We found that aged Rhoh$^{-/-}$ (KO) mice had shortened lifespans and developed B cell derived splenomegaly with an increased Bcl-6 expression profile in splenocytes. We utilized a murine model of Bcl-6 driven DLBCL to further explore the role of RhoH in malignant behaviour by crossing Rhoh^{KO} mice with Iμ-HABcl-6 transgenic (Bcl-6^{Tg}) mice. The loss of Rhoh in Bcl-6^{Tg} mice led to a more rapid disease progression. Mechanistically, we demonstrated that deletion of Rhoh in these murine lymphoma cells was associated with decreased levels of the RhoH binding partner KAISO, a dual-specific Zinc finger transcription factor, de-repression of KAISO target Bcl-6, and downregulation of the BCL-6 target Blimp-1. Re-expression of RhoH in Rhoh^{KO}Bcl-6^{Tg} lymphoma cell lines reversed these changes in expression profile and reduced proliferation of lymphoma cells in vitro. These findings suggest a previously unidentified regulatory role of RhoH in the proliferation of tumour cells via altered BCL-6 expression. (250)

ARTICLE HISTORY
Received 12 August 2021
Revised 3 December 2021
Accepted 13 December 2021

KEYWORDS
RhoH; KAISO; BCL-6; Blimp-1; lymphoma; malignant transformation; B cells

Introduction

Rho GTPases are guanine nucleotide-binding proteins that cycle between an active GTP-bound state and an inactive GDP-bound state. As such, they have key roles in the modulation of a wide range of cellular processes including proliferation, apoptosis, cell migration, cell polarization, membrane trafficking, cytoskeleton rearrangements, and transcriptional regulation [1].

RhoH, a haematopoietic-specific and GTPase-deficient RhoGTPase, was first identified as a hypermutable gene and translocation partner in human Diffuse Large B-Cell Lymphoma (DLBCL) and was initially named *Translocation Three Four (TTF)* [2–4]. This atypical Rho GTPase lacks intrinsic GTPase activity and remains in a constitutively active, GTP-bound state [2,5]. In addition, it contains a functional immunoreceptor tyrosine-based activation motif (ITAM)-like motif [6]. Thus, RhoH cellular function is likely related to its level of expression, intracellular localization, and phosphorylation state [6–11]. RhoH antagonizes Rac1 in regulating F-actin assembly and chemotaxis in haematopoietic stem/progenitor cells (HSPCs) by reducing Rac1 membrane targeting and activation, and this regulation is mediated by C-terminal sequences, including a CKIF motif, which is a C-terminal RhoH-specific motif of four amino acids (Cysteine, Lysine, Isoleucine, and Phenylalanine) [12]. *Rhoh*-deficient (*Rhoh*^{KO}) haematopoietic cells

CONTACT David A. Williams DAWilliams@childrens.harvard.edu Division of Hematology/Oncology, Boston Children's Hospital, 300 Longwood Ave. Karp 08125.3, Boston, MA 02115, USA
*These authors contributed equally to this work.
Supplemental data for this article can be accessed here.

exhibit abnormal random migration [7]. In T cells, RhoH is required for CD3-zeta phosphorylation and recruitment of the protein tyrosine kinases Zap70 and Lck to the cellular membrane and immunologic synapse [6]. *Rhoh*^{KO} mice exhibit a T cell deficiency due to impaired T cell receptor-mediated selection and maturation of thymocytes. However, these mice show only minor alterations in B cell development and *in vitro* function [9].

RHOH mutations have been reported in 35 of 100 DLBCL cases [13] and mutations of the 5′-noncoding region and first intron of the *RHOH* gene have been found in a variety of B lymphoid malignancies, including DLBCL [4]. In particular, aberrant somatic hypermutation (SHM) in the 5′ untranslated region of the *RHOH* gene has been detected in DLBCL. However, the effect of *RHOH* mutations and translocations on RhoH expression and the biology of lymphoma are currently unknown. Recent findings of abnormal RhoH expression levels in haematological malignancies further suggest that it may play an important role in malignant transformation and progression. Under-expression of RhoH has been shown to correlate with disease progression and decreased survival in Acute Myeloid Leukaemia (AML) [12], while constitutively active Rac1 has been demonstrated to inhibit apoptosis in human lymphoma cells by stimulating Bad phosphorylation [14]. Therefore, it is possible that decreased expression of RhoH may lead to increased protection of leukaemia cells from apoptosis via Rac1 inhibition [12] and contribute to chemotherapy resistance.

In this study, we demonstrate that *Rhoh*^{KO} mice have decreased lifespans and develop features of lymphoma including enlarged spleens with expanded CD19^{+} B cell populations that exhibit increased levels of BCL-6 and Ki-67 expression when compared with wild type (*WT*) mice. To better define the effects of dysregulated RhoH on lymphoma development, we generated *Rhoh*-deficiency in a DLBCL mouse model by interbreeding *Rhoh*^{KO} mice with *Iμ-HABcl-6, Bcl-6*^{Tg} mice that constitutively express BCL-6 in B cells. We report that loss of RhoH is associated with a more aggressive disease phenotype in this mouse model and *Rhoh*-deficient *Bcl-6*^{Tg} lymphoma cells show a higher proliferative activity compared with *WT* cells. Mechanistically, we demonstrate binding of RhoH and KAISO, a dual function zinc finger transcriptional repressor of *Bcl-6*, and show decreased cellular content of KAISO in the absence of RhoH in lymphoma cells. This decreased protein level is associated with de-repression of endogenous *Bcl-6* and downregulation of the BCL-6 target gene *Blimp-1*, deficiency of which is associated with an aggressive phenotype in DLBCL. Our results therefore contribute new understanding to the potential role of deregulated RhoH expression levels in the development of *Bcl-6*-driven lymphoma.

Materials and methods

Mice

The generation of the *Rhoh*^{KO} mouse model on a C57BL/6J background has been described previously [6]. The *Bcl-6*^{Tg} mouse model with a C57BL/6 J background was kindly provided by Dr. Laura Pasqualucci. The *Rhoh*^{WT}*Bcl-6*^{Tg} *(WTTg)* animals were generated by breeding *Rhoh*^{WT} mice with *Bcl-6*^{Tg} mice, and the *Rhoh*^{KO}*Bcl-6*^{Tg} (*KOTg*) mice were generated by breeding *Rhoh*^{KO} mice with *Bcl-6*^{Tg} mice.

Vector constructs

The mouse stem cell virus (MSCV)–based retroviral vector with yellow fluorescent protein (YFP) and 3x-haemagglutinin-(HA)-tagged wild-type mouse RhoH cDNA (HA–RhoH) [15] was used to transduce *Rhoh*^{KO}*Bcl-6*^{Tg} (*KOTg*) B cell lymphoma and *Rhoh*^{KO}*Bcl-6*^{nTg} (*KOnTg*) B cell malignant cell lines. A FLAG-tagged wild-type mouse *Blimp-1* cDNA was subcloned into an enhanced green fluorescent protein (EGFP) expressing modified MSCV-based retroviral vector, MIGR1 (Addgene Plasmid # 27,490, Watertown, MA), at XhoI and EcoRI restriction sites. This vector (FLAG-BLIMP-1) was used for the transduction of the *KOTg* B cell lymphoma cell line (see Supplemental Figure S1).

Establishment of murine lymphoma cell lines, cell culture and transduction

To establish *Rhoh*^{KO}*Bcl-6*^{Tg} (*KOTg*) lymphoma cell lines with both endogenous and exogenous BCL-6 expression and a *Rhoh*^{KO}*Bcl-6*^{nTg} (*KOnTg*) malignant B cell line with lymphoma characteristics having only endogenous BCL-6 expression, CD19^{+} cells were isolated from enlarged spleens of animals diagnosed with B cell lymphoma or with enlarged spleens and expanded CD19^{+} cells, respectively, by pathological examination. The cells were then cultured in RPMI1640 (Cytiva Hyclone Laboratories, South Logan, UT) with 20% foetal bovine serum (Sigma, St. Louis, MO) and 100 mM of 2-mercaptoethanol (Sigma) *in vitro*. After 2–3 weeks in culture, these lymphoma and B cell-derived cell lines were cryopreserved and a subculture passaged serially. The surface expression of CD19 on these cell lines was

confirmed by fluorescence activated cell sorter (FACS) analysis.

Histology preparations

Spleens from mice were formalin-fixed and paraffin-embedded. On serial histological sections, haematoxylin and Eosin (H&E) staining and immunohistochemistry staining were performed at the Rodent Histopathology Core Facility or Brigham and Women's Hospital Pathology Core Facility using standard protocols.

Flow cytometry analysis

For flow cytometry analysis, the following fluorescence-labelled antibodies were used: Ki-67-PE (20 µL per reaction), which was purchased from BD Biosciences, San Jose, CA, and CD19-FITC (6D5, 1:100), which was obtained from BioLegend, San Diego, CA. Ki-67 staining was conducted according to the manufacturer's recommendations. Cells were analysed on a LSRFortessa flow cytometer (BD Bioscience) using BD FACSDiva software.

Immunoprecipitation and immunoblotting

Primary $CD19^+$ B cells of wild-type non-transgenic (*WTnTg*), wild-type transgenic (*WTTg)*, and Rhoh *KO* transgenic (*KOTg)* spleens were isolated using magnetic beadsconjugated with CD19 antibody (90 µL per 10^7 cells) and an autoMACS Pro separator (Miltenyi Biotec, Bergisch Gladbach, Germany) according to the manufacturer's recommendations. The purity of the isolated $CD19^+$ cells was more than 90% as determined by flow cytometry.

To obtain whole-cell lysates, RIPA buffer (10 mM TrisHCl pH 7.4, 130 mM NaCl, 1% Triton X-100, 0.1% sodium dodecyl sulphate (SDS), 0.5% sodium deoxycholate) containing protease (Complete Protease Inhibitor Cocktail, Roche Applied Science, Indianapolis, IN) was used to lyse the isolated cells. The cytoplasmic and nuclear proteins were extracted separately using NE-PER nuclear and cytoplasmic extraction reagents (Pierce Biotechnology, Rockford, IL, USA) according to the manufacturer's protocol.

For immunoprecipitation, the cells were lysed in 1X cell lysis buffer (20 mM Tris-HCl (pH 7.5), 150 mM NaCl, 1 mM Na_2EDTA, 1 mM EGTA, 1% Triton, 2.5 mM sodium pyrophosphate, 1 mM β-glycerophosphate, 1 mM Na_3VO_4, 1 µg/ml leupeptin) (Cell Signalling Technology, Danvers, MA). The cell lysates were subjected to immunoprecipitation with anti-HA monoclonal antibody (1:100) (Thermo Scientific, Waltham, MA) followed by Protein A Magnetic Bead isolation (Cell Signalling Technology).

Western blotting was done following standard procedures and transferred onto PVDF membranes. The following primary antibodies were used: anti-BCL-6 (Cell Signalling Technology, 1:1000), anti-BLIMP-1 (BioLegend, 1:100 or Cell Signalling Technology, 1:250), anti-KAISO (Abcam, Cambridge, MA, 1:1000), anti-HA (Thermo Scientific, Waltham, MA, 1:1000), anti-Lamin B (Abcam, 1:1000), anti-Tublin A (Abcam, 1:1000), and anti-β-actin (Thermo Scientific, Waltham, MA, 1:5000 or 1:20,000). The sheep anti-mouse IgG (1:3000) or the anti-rabbit IgG (1:3000) horseradish peroxidase linked antibodies from Cell Signalling Technology were used as secondary antibodies and ECL reagent (Super Signal West Pico, Thermo Scientific, Rockford, IL) was used for detection.

Indirect immunofluorescence

Cells were layered onto poly-L-lysine coated slides and subsequently fixed with 4% paraformaldehyde and permeabilized with PBS–0.2% Triton X-100 for 5 minutes at room temperature. Fixed cells were blocked with 2% bovine serum albumin (Sigma) in PBS at room temperature for 1 hour, then incubated with anti-KAISO antibody (Abcam, 1:500) overnight at 4°C, followed by a 50-minute incubation with Alexa Fluor® 647 (1:500) conjugated anti-mouse IgG antibody (Cell Signalling Technology). Coverslips were mounted with ProLong Glass Antifade Mountant with NucBlu Stain (Thermo Fisher Scientific, Waltham, MA), and images were captured using a laser confocal microscope (Leica TCS SP8 (STED One) Scanning Confocal-Microscope, Wetzlar, Germany) with 100X magnification.

Chromatin immunoprecipitation (ChIP-qPCR)

ChIP was performed as previously described [16]. Briefly, cells were fixed in 1% formalin (v/v) in PBS with gentle rotation for 10 minutes at room temperature. Fixation was stopped by the addition of 125 mM glycine. Fixed cells were washed twice in ice-cold PBS and resuspended in sodium dodecyl sulphate (SDS) lysis buffer (1% SDS, 10 mM EDTA, 50 mM Tris-HCl, pH 8.1). Chromatin was sheared by sonication to about 100–500bp fragments using Bioruptor (Diagenode, Denville, NJ) and diluted ten-fold with dilution buffer (0.01% SDS, 1.1% Triton-X100, 1.2 mM EDTA, 16.7 mM Tris-HCl, pH8.1,167 mM

NaCl). Antibody against KAISO (Abcam, 8 μg per reaction) was used to precipitate DNA fragments associated with KAISO. Precipitates were washed sequentially with ice cold low salt wash (0.1% SDS, 1% Triton-X-100, 2 mM EDTA, 20 mM Tris-HCl, pH8.1, 150 mM NaCl), high salt wash (0.1% SDS, 1% Triton-X-100, 2 mM EDTA, 20 mM Tris-HCl, pH 8.1, 500 mM NaCl), LiCl wash (0.25 M LiCl, 1% IGEPAL CA-630, 1% deoxycholic acid, 1 mM EDTA, 10 mM Tris-HCl, pH 8.1), and TE wash (1 mM EDTA, 10 mM Tris-HCl, pH 8.1) and finally eluted in elution buffer (1% SDS, 0.1 M NaHCO3). All buffers except for the elution buffer were supplemented with protease inhibitors (Complete Mini Protease Inhibitor Cocktail tablets, Roche). Eluted DNA fragments were analysed by quantitative PCR using promoter specific primers as listed.

RNA extraction and real-time PCR

Trizol (Invitrogen, Carlsbad, CA) was used to extract RNA from viable cells. Polymerase chain reaction (PCR) master mixes were used (SYBR Green, Applied Biosystems, Grand Island, Ny), and real-time PCR was performed using the 7500 Real-Time PCR System (Applied Biosystems). Further assay details can be provided on request.

Statistics

Microsoft Excel and GraphPad Prism software were used for statistical analysis. Statistical significance between two groups was determined by unpaired 2-tailed Student's *t*-test. The Kaplan–Meier method was used to plot survival curves for murine B cell lymphoma mice, and the log-rank test was used to evaluate statistical differences. A *p*-value less than 0.05 was considered significant. Image J software from NIH was used for Western blot quantification.

Study approval

All animal experiments described in this study were approved by and adhered to the guidelines of the Institutional Animal Care and Use Committee of Boston Children's Hospital. (Protocol number: 17–01-3365)

Results

Rhoh$^{-/-}$ (KO) mice have shortened lifespans and splenomegaly due to an expansion of proliferating B cells with increased BCL-6 expression

Although *Rhoh* deletion *(KO)* had only a modest effect on B cell development in mice [9], we observed these animals had shortened lifespans when compared to *WT* mice (562 days vs 692 days; *KO* vs *WT*, median survival, $p < 0.01$) (Figure 1(a)) that was associated with increased spleen weight in *KO* mice early in life (Figure 1(b)). Spleen histology showed prominent expansion of the white pulp areas with effacement of the structure due to a diffuse proliferation of medium-large lymphoid cells in *KO* mouse spleens. Immunohistochemistry demonstrated that the expanded cells were mostly CD19^{+} B cells with increased percentages of BCL-6 and Ki-67 positive cells in the absence of *Rhoh* when comparing *WT* and *KO* mouse spleens (Figure 1(c)). The abnormal spleen architecture and the significantly increased percentage of Ki-67^{+} cells in the *KO* mouse spleen compared to the *WT* control (Figure 1(d)) suggest that splenomegaly was likely due to increased proliferation of B lymphoma cells. The role of RhoH in the increased proliferation was confirmed using a B cell line derived from the enlarged spleen of this *KO* mouse. RhoH was re-expressed in these cells using retrovirus-mediated gene transfer. RhoH re-expression significantly decreased cell proliferation of these *KO* mouse cells (Figure 1(e)). These data imply that RhoH deficiency may be linked to an expansion of B cells in primary mice that is associated with reduced lifespan of *KO* mice.

Rhoh^{KO}*Bcl-6*^{Tg} mice show more rapid disease progression in a murine model of lymphoma with increased proliferation of lymphoma cells

To further examine the potential role of RhoH in dysregulated B cell development and lymphomagenesis, we crossed *WT* and *KO* mice with the *Iμ-HABcl-6* transgenic (*Bcl-6*^{Tg}) DLBCL mouse model [17]. In this mouse model, a HA-tagged full length murine BCL6 coding sequence was inserted into the downstream of the immunoglobulin heavy chain (IgH) Iμ promoter on mouse chromosome 12 in murine ES cells. The recombinant locus can produce a chimeric mRNA (Iμ-HABCL6) whose transcription is driven by the Iμ promoter, which is detected in both the germinal centre (GC) and plasma cells of IμHABCL6 mice [17]. The resulting *Rhoh*^{KO}*Bcl-6*^{Tg} (*KOTg*) and *Rhoh*^{WT}*Bcl-6*^{Tg} (*WTTg*) mice were observed for disease development. *KOTg* mice died more quickly than *WTTg* mice (Figure 2(a), Table 1) and this premature death was associated with development of severe splenomegaly more rapidly (Figure 2(b,c)). Diseased *WTTg* and *KOTg* mice displayed loss of splenic architecture and invasion of spleen parenchyma by large, heterogenous lymphoid cells resembling human DLBCL cells (Figure 2(d)). In contrast to *WTTg* mice, immunohistochemistry revealed that *KOTg* lymphoma cells had even higher BCL-6 expression and were uniformly and strongly positive for IRF4, suggesting that loss of RhoH alters the phenotype of

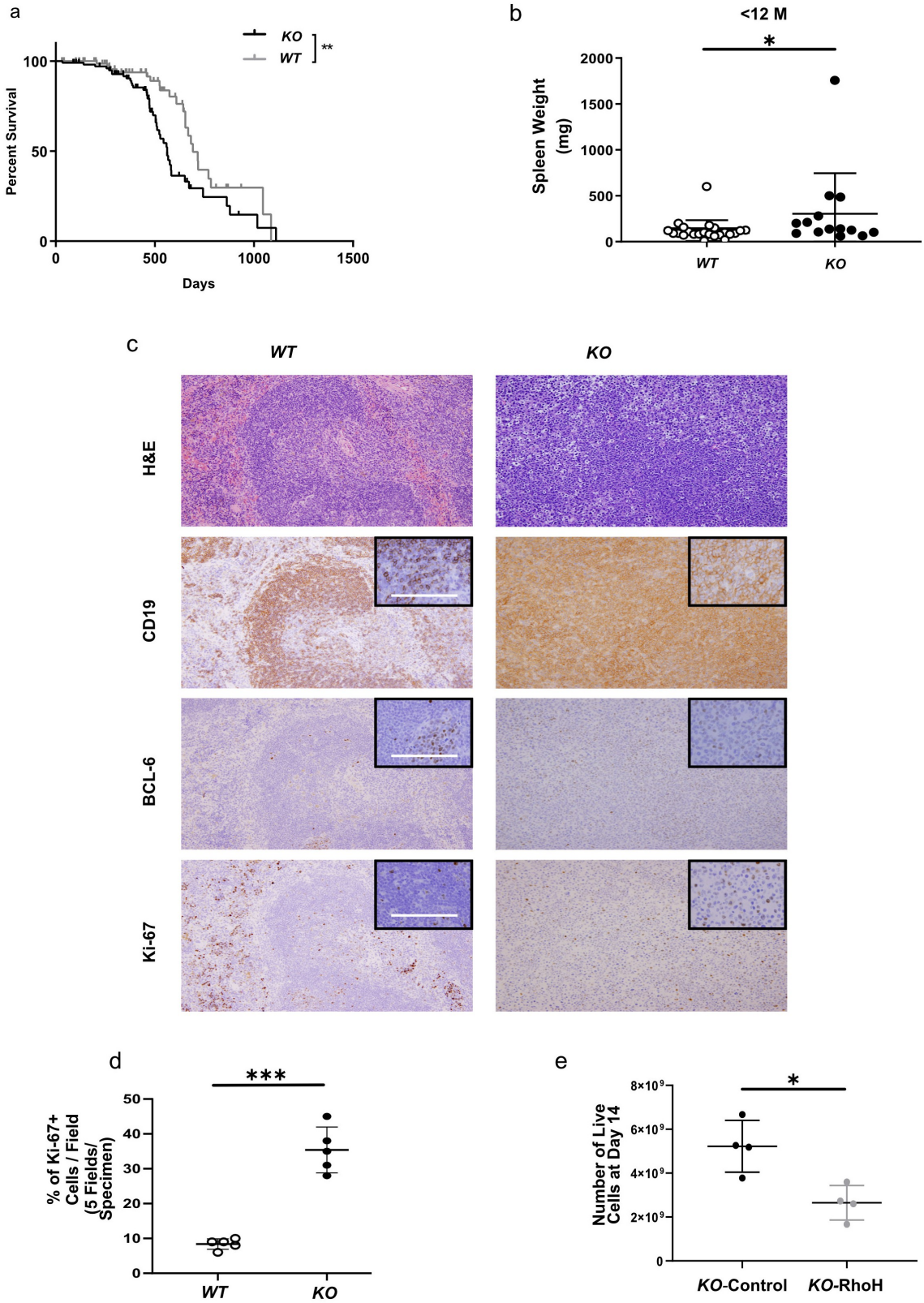

Figure 1. *KO* mice have splenomegaly and increased BCL-6 expression in B cells compared with *WT* mice; and RhoH re-expression decreases proliferation of *KO* mouse cells with lymphoma characteristics. (a) Survival curves of *WT* and *KO* mice, n = 66 and 65 respectively. **p < 0.01, Log-rank test. (b) Spleen weights of *WT* and *KO* mice under 12 months-age, n = 23 and 12, respectively. (c) Photomicrograph of representative sections from spleens of age-matched *WT* and *KO* mice stained with haematoxylin and eosin (H&E) (20X magnification); and immunohistochemistry stains with anti-CD19, anti-BCL-6, and anti-Ki-67 antibodies (20X; inset: 100X magnification). Scale bars are 100 µm. (d) Percentage of Ki-67 positive cells in the white pulp areas of *WT* spleen *versus KO* spleen as determined by immunohistochemistry (each value is an average of the percentage of Ki-67 positive cells calculated in 5 different areas in each sample; n = 4). (e) *In vitro* growth of *KO* $CD19^{+}$ B cell line transduced with RhoH-expressing retrovirus vector (*KO*-RhoH) *versus* empty vector (*KO*-Control), n = 4. Data show mean ± SD. * p < 0.05, *** p < 0.0001.

lymphoma at the cellular level according to Hans criteria [18] to a more aggressive phenotype in the *Iμ-HABcl-6* transgenic (*Bcl-6*^{Tg}) DLBCL mouse model. We next compared proliferation and apoptosis of *WTTg* and *KOTg* lymphoma cells. The percentage of Ki-67-positive cells was significantly increased in *KOTg* splenic lymphoma cells compared to *WTTg* lymphoma controls (Figure 2(e)). In contrast, there was no significant difference in the rate of apoptosis as measured by Cleaved Caspase-3 (CC3) (Figure 2(f,g)). Taken together, these results reveal that deletion of *Rhoh* is associated with a more aggressive disease phenotype in this *Bcl-6*-driven lymphoma mouse model, with increased proliferation of lymphoma cells.

RhoH interacts with KAISO and affects the cellular content of KAISO, expression of its target Bcl-6, and downregulation of the BCL-6 target Blimp-1 in lymphoma cells

We have previously reported that RhoH interacts and co-localizes in the nucleus with KAISO, a dual-specific, Broad complex, Tramtrak, Bric-a-brac/Pox virus, Zinc finger (POZ-ZF) transcription factor [19]. In addition, knockdown of RhoH leads to decreased nuclear localization of KAISO in Jurkat T cells [19]. KAISO has also been shown to act as a key regulator of spleen germinal centre (GC) formation by repressing *Bcl-6* expression in splenocytes [20]. As KAISO knockout mice develop splenomegaly and large diffuse germinal centres associated with increased expression of *Bcl-6* and *c-Myc*, we hypothesized that the increased expression of BCL-6 seen in *KOTg* lymphoma cells could be related to decreased nuclear content of KAISO in the absence of RhoH. Immunoblot analysis showed decreased KAISO protein expression in the whole cell lysates of *KOTg* lymphoma cells when compared with *WTTg* lymphoma cells (Figure 3(a,b)). Using fractionated lysates isolated from *WTTg* and *KOTg* lymphoma cells, we performed immunoblot analysis to examine the expression of KAISO in those fractions. While nuclear KAISO was decreased in *KOTg* lymphoma cells compared to *WTTg* lymphoma cells (Figure 3(a,b)), cytoplasmic KAISO was not significantly different in these cells (Figure 3(a,b)). In order to confirm that KAISO and RhoH interact in this lymphoma model, we re-expressed RhoH in B cells derived from *KOnTg* mice cells using retrovirus-mediated gene transfer. As seen in (Figure 3(c)), HA-tagged RhoH bound to KAISO in RhoH-transduced *Rhoh*^{KO} B cells, confirming the interaction of KAISO and RhoH in those cells using co-immunoprecipitation.

To test whether the re-expression of RhoH can affect the cytoplasmic and nuclear distribution of KAISO, B cell lymphoma cell lines established from enlarged spleens of *KOTg* mice were transduced with a retrovirus vector expressing HA-tagged RhoH. With immunoblot analysis from the whole cell lysates, we first show that RhoH re-expression increases the total protein expression of KAISO in the *KOTg*-RhoH cells compared to the *KOTg* control cells (Figure 3(d,e)). Then, using the isolated fractionated lysates, we show that RhoH re-expression increased the level of KAISO in both the cytoplasm and nucleus of *KOTg*-RhoH cells compared to *KOTg* control cells (Figure 3(d,e)). The increased amount of KAISO protein in *KOTg*-RhoH cells was further confirmed by immunofluorescence staining (Figure 3(f)). Together, these data provide evidence that the interaction between RhoH and KAISO affects the protein levels of the transcription factor KAISO.

As noted above, direct repression of *Bcl-6* by KAISO has been reported previously in germinal centre splenocytes, and de-repressed *Bcl-6* expression was associated with an increased proliferation of GC cells and splenomegaly in KAISO knockout mice [20]. To further test whether the up-regulation of BCL-6 protein expression observed in *KOTg* lymphoma cells was due to the release of KAISO-mediated suppression of *Bcl-6*, we performed a KAISO ChIP assay in *KOTg* lymphoma cells transduced with RhoH (RhoH). ChIP-qPCR analysis revealed a significant enrichment of KAISO binding at R1 (bp, −900~-450) and R3 (bp, +2165~+2423), two regulatory regions of the *Bcl-6* promoter, in the *KOTg*-RhoH cells compared to *KOTg* control cells (Figure 4(a)). In contrast, no significant enrichment of the KAISO binding was detected at the *Flt3* gene locus in the *KOTg*-RhoH cells used as a negative control compared to *KOTg* control cells, suggesting the binding of KAISO at the *Bcl-6* promoter was specific. These results strongly indicate that lack of KAISO occupation at the *Bcl-6* promoter region may directly de-repress the transcription of the *Bcl-6* gene.

BCL-6 has been shown to directly repress expression of the transcription factor *BLIMP-1* [21,22] and deficiency of BLIMP-1 was demonstrated to interfere with the differentiation of B cells into plasma cells [23]. We conducted immunoblot analysis of whole cell or fractionated cell lysates isolated from primary *WTTg* and *KOTg* lymphoma cells to analyse the expression of BCL-6. BCL-6 protein expression was consistently increased especially in the nucleus of sorted CD19^{+} *KOTg* lymphoma cells compared with *WTTg* lymphoma controls (Figure 4(b,c)). Immunoblot analysis of BLIMP-1 indicated that the expression of BLIMP-1 in whole cell lysates was consistently reduced in *KOTg* lymphoma cells compared to normal B cells or *WTTg*

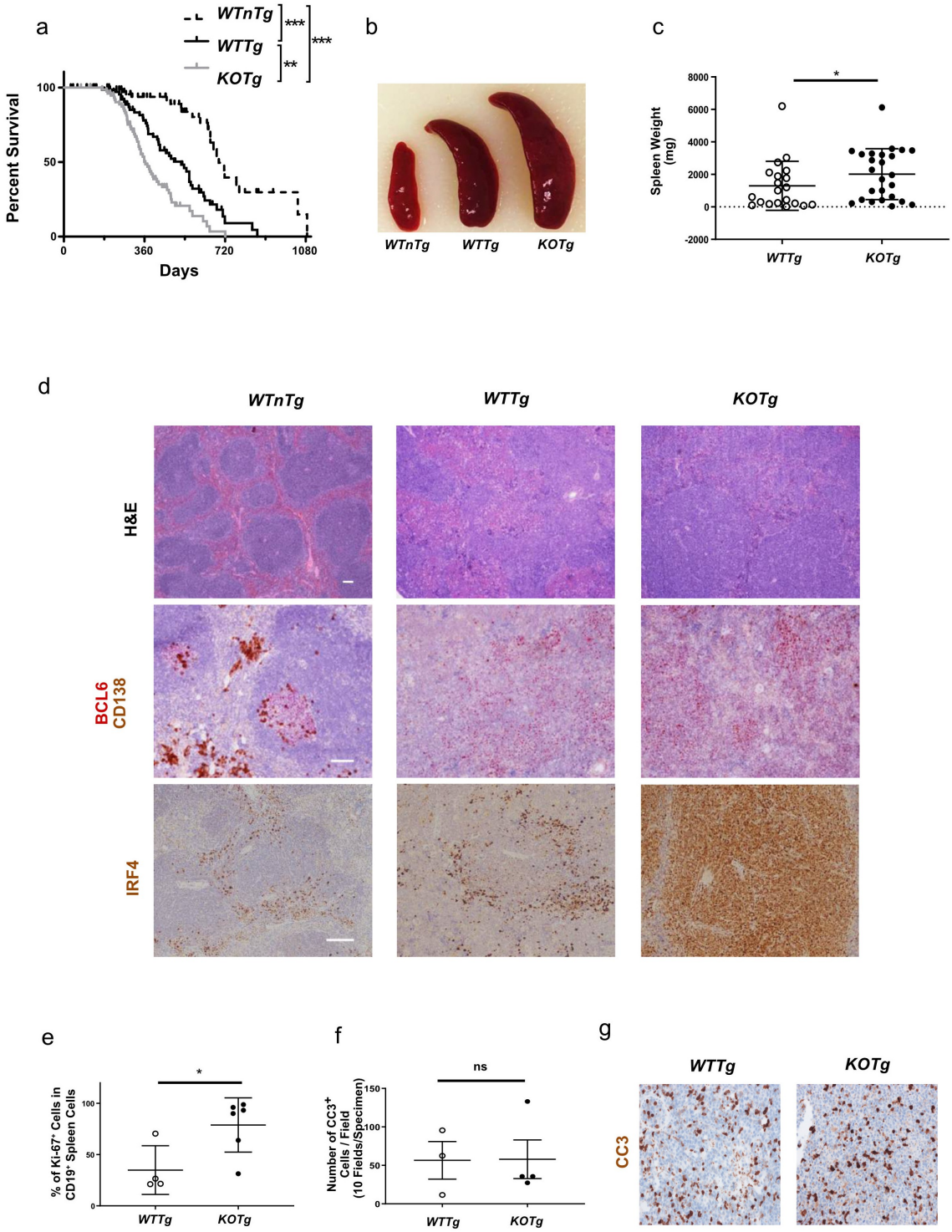

Figure 2. *KOTg* mice show significantly shorter lifespans, increased splenomegaly, and increased lymphoma cell proliferation compared with *WTTg* mice. (a) Survival curves of *WTnTg, WTTg*, and *KOTg* mice, n = 82, 67, and 69 respectively. ** $p < 0.01$, *** $p < 0.001$, Log-rank test. (b) Representative photographs of spleens of age-matched *WTnTg, WTTg*, and *KOTg* mice. (c) Spleen weights of *WTTg* and *KOTg* mice with lymphoma at pre-terminal stage, n = 20 and 25, respectively. (d) Photomicrograph of representative sections from spleens of *WTnTg, WTTg*, and *KOTg* mice stained with haematoxylin and eosin (H&E) (40X magnification); and immunohistochemistry stains with anti-BCL-6 and anti-CD138 or anti-IRF4 antibodies (100X magnification). Scale bars are 100 µm. (e) The percentage of Ki-67^+ $CD19^+$ lymphoma cells in *WTTg* (n = 4) and *KOTg* (n = 6) spleens as determined by flow cytometry. (f) Number of Cleaved Caspase-3 $(CC3)^+$ lymphoma cells derived from *WTTg* and *KOTg* spleens as determined by immunohistochemistry, n = 3 and 4, respectively. (g) Photomicrograph of representative sections from spleens of *WTTg* and *KOTg* mice immunohistochemistry stained with anti-CC3 antibody. For (c), (e) and (f), data show mean ± SD; student t-test was used for data analysis: * $p < 0.05$; ns: no significant difference.

Table 1. Median survival of *WTnTg, WTTg*, and *KOTg* mice.

Median survival (Days)	
WTnTg	718
WTTg	492
KOTg	359

n = 82, 67, and 69, respectively.
a. $p < 0.001$, Log-rank test comparing survival for *WTnTg* mice with *WTTg* mice.
b. $p < 0.001$, Log-rank test comparing survival for *WTnTg* mice with *KOTg* mice.
c. $p < 0.01$, Log-rank test comparing survival for *WTTg* mice with *KOTg* mice.

lymphoma cells (Figure 4(d,e)). These data further support that absence of RhoH is associated with decreased expression of *Blimp-1*, an important gene for the terminal differentiation of B cells to plasma cells in this murine model.

Higher expression of BCL-6 and decreased expression of BLIMP-1 associated with Rhoh deficiency can be reversed by RhoH re-expression

Restoration of RhoH expression in *Rhoh*-deficient *KOTg* lymphoma cells using gene transfer led to reduced overall BCL-6 expression (Figure 5(a)) in these cells compared to *KOTg* controls. BCL-6 expression assessed by anti-BCL-6 antibody in lymphoma cells derived from *Iμ-HABcl-6* transgenic mice detects both the transgenic HA tagged-BCL-6 protein and endogenous BCL-6 protein. Since HA-BCL-6 expression detected by anti-HA antibody was similar between *KOTg* and *KOTg*-RhoH cells (Figure 5(a,b)) and we had previously demonstrated increased BCL-6 expression in the spleens of *KO* mice (Figure 1(c)), we surmised that increased expression of BCL-6 in *KOTg* lymphoma cells was mainly the result of changes in endogenous *Bcl-6* gene expression. This was confirmed using B cells derived from *KOnTg*-RhoH mice, which lack expression of transgenic *Bcl-6*. Re-expression of RhoH in *KOnTg*-RhoH B cells was associated with decreased BCL-6 protein levels detected by immunoblot analysis (Figure 5(c,d)) and decreased *Bcl-6* mRNA expression by quantitative RT-PCR (qRT-PCR) (Figure 5(e)). Accordingly, the expression of BLIMP-1, a direct target of BCL-6 repression, was increased in *KOnTg*-RhoH cells compared to *KOnTg* controls (Figure 5(c,f)), suggesting that the re-expression of RhoH affects not only endogenous *Bcl-6* expression but also the expression of genes regulated by BCL-6. Overall, these results indicate that RhoH deficiency leads to deregulated BCL-6 expression that can be partially reversed by the re-expression of RhoH and that in this lymphoma model, RhoH affects BCL-6 transcription through a transcription cascade via RhoH interacting protein KAISO, which is a repressor of BCL-6.

Re-expression of RhoH in lymphoma cells reduces proliferation in vitro

To implicate RhoH deficiency in the increased cellular proliferation seen *in vivo*, we re-expressed RhoH in *KOTg* lymphoma cells using retrovirus-mediated gene transfer. Re-expression of RhoH in *KOTg* lymphoma cells led to significantly decreased proliferation measured after 7-days in culture ($8.6x10^6 \pm 1.9x10^5$ cells vs $5.9 \times 10^6 \pm 1.9x10^5$ cells; *KOTg*-Control vs *KOTg*-RhoH, mean ± SD, $p < 0.05$) (Figure 6(a)). Growth after subsequent days in culture was consistently significantly different as observed through 14 days (Supplemental Figure S2). These results indicate that RhoH regulates proliferation in *Bcl-6*-driven lymphoma cells. We next determined the contribution of decreased expression of BLIMP-1, which is also altered in *Rhoh* deficient cells, to increased proliferation of the lymphoma cells. We over-expressed BLIMP-1 in these *KOTg* lymphoma cells using retrovirus-mediated gene transfer. Over-expression of BLIMP-1 led to significantly decreased cell proliferation measured after 6-days in culture ($1.3x10^6 \pm 7.4x10^4$ cells vs $1.8 \times 10^5 \pm 1.0x10^4$ cells; *KOTg*-Control vs *KOTg-BLIMP-1*, mean ± SD, $p < 0.001$) (Figure 6(b,c)). Growth was observed to be consistently significantly different through 10 days in culture (Supplemental Figure S2). Overall, our results suggest that the rescue of RhoH expression and the resulting increased expression of the BCL-6 downstream target in this transcriptional cascade, BLIMP-1, may reverse the disease phenotype in *KOTg* mice.

Discussion

RhoH is a haematopoietic-specific, GTPase-deficient member of the Rho (Ras homology) family of small GTPases. RhoH was originally discovered as a translation partner of LACZ/BCL-6 and termed Translocation Three Four (TTF) [3] and also found to be mutated in a number of B cell lymphomas [13]. In humans, loss of function mutations of *RHOH* have been associated with *Epidermodysplasia Verruciformis* related to abnormal T lymphocyte phenotype and function [24]. In mice, loss of *Rhoh* is associated with lack of proper thymic T cell selection and T cell lymphopenia, due to defective proximal T cell receptor signalling, whereas B cell development appears relatively normal [6,25]. While implicated in both immunological function and in various haematologic malignancies, the role of RhoH in tumour development is not clear. For instance, mutations in the *RHOH* non-coding regions in B cell malignancies

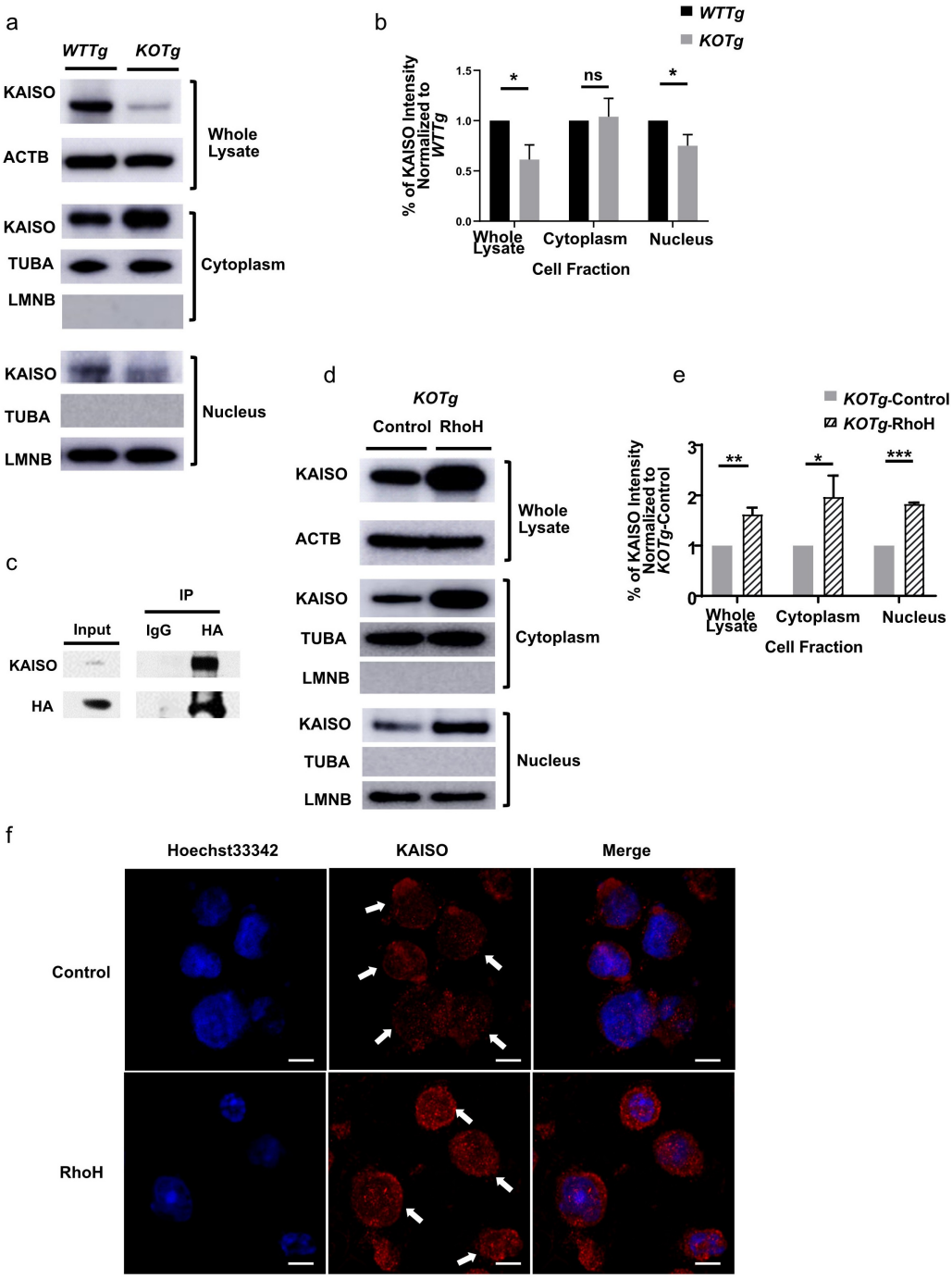

Figure 3. RhoH interacts with KAISO and deletion of *Rhoh* is associated with decreased nuclear content of KAISO in lymphoma cells. (a) Western blot analysis showing the expression of KAISO in the whole cell lysates (top panel), cytoplasmic (middle panel) and nuclear (lower panel) fractions of sorted CD19^{+} spleen cells isolated from *WTTg* and *KOTg* mice. (b) Intensity of KAISO Western blot bands by Image J analysis in the whole cell lysates, cytoplasmic, and nuclear fractions of sorted CD19^{+} spleen cells isolated from *WTTg* and *KOTg* mice. KAISO band intensity is normalized to the internal control, and those values are normalized to the *WTTg* KAISO internal control normalized values, n = 3. (c) Western blot analysis of immunoprecipitation of whole cell lysates from a malignant *KOnTg* B cell line transduced with a retroviral vector expressing HA-RhoH (HA-RhoH) using an anti-HA monoclonal antibody or IgG control followed by immunoblotting with anti-KAISO monoclonal antibody. (d) KAISO protein expression by Western blot analysis in the whole cell lysates (top panel), cytoplasmic (middle panel), and nuclear (lower panel) fractions of a *KOTg* lymphoma cell line transduced with empty vector (Control) or HA-RhoH (RhoH). (e) Intensity of KAISO Western blot bands by Image J analysis in the whole cell lysates, cytoplasmic, and nuclear fractions of a *KOTg* lymphoma cell line transduced with empty vector (Control) or HA-RhoH (RhoH). For (a), (b), (d) and (e), β-Actin (ACTB) was used as a loading control for whole cell lysates, α-TUBULIN (TUBA) and LAMIN B1 (LMNB) were used as loading controls for cytoplasmic and nuclear fractions, respectively. KAISO band intensity is normalized to these internal controls, and those values are normalized to the *KOTg*-Control KAISO internal control normalized

may be associated with reduced expression, and decreased expression of RhoH has been shown to predict poorer outcomes in AML, chronic lymphoid leukaemia (CLL) and Hairy Cell Leukaemia [8,26]. In some cases, it has been hypothesized that the pathogenesis is related to the lack of RhoH inhibition of Rac1 and downstream effectors, including phosphoinositol-3-kinase and the Rho guanine exchange factor VAV1, or effects on myeloid differentiation. In contrast, in some instances increased expression of RhoH has been noted in leukaemia cells, specifically in CLL [9], and RhoH deficiency in a murine model of CLL reduced accumulation of leukaemic cells. Thus, the role(s) of RhoH in transformation of haematopoietic cells remains incompletely understood.

In this study, we provide direct evidence that RhoH regulates a transcription pathway modulating the expression of BCL-6 associated with expansion of B cell populations over time *in vivo*, resulting in a reduced lifespan of $Rhoh^{-/-}$ (*KO)* mice. Further, in a model of BCL-6 dependent B cell malignancy, we demonstrate that genetic loss of *Rhoh* leads to a more rapid disease progression with increased proliferation of lymphoma cells. Mechanistically, the deletion of *Rhoh* in these lymphoma cells is associated with reduced expression of the RhoH binding partner KAISO, which is associated with the derepression of *Bcl-6*, a known KAISO target, and down-regulation of the BCL-6 target *Blimp-1* (Figure 6(d)). Re-expression of RhoH in $Rhoh^{KO}Bcl\text{-}6^{Tg}$ (*KOTg*) lymphoma cell lines increases nuclear KAISO levels, decreases BCL-6 protein expression, and leads to reduced proliferation of lymphoma cells. These data suggest that RhoH plays an important role in KAISO mediated transcriptional repression of *Bcl-6*, a major regulator of B cell development.

We previously demonstrated that RhoH participates in a multi-protein complex with KAISO in Jurkat T cells [19]. KAISO has been defined as a dual-function DNA-binding transcription factor and binds to both methylated CpG dinucleotides in the consensus sequence 5′-CGCG-3′ and sequence-specific KAISO binding sites (KBS, 5′-CTGCNA-3′) within target gene promoters through its C-terminal zinc-finger motif [27–29]. Therefore, endogenous KAISO protein levels in the nucleus of mammalian cells is critical for its role in gene regulation [30,31]. Although KAISO has been shown to activate transcription of a subset of target genes [32–34], the predominant role of KAISO is considered to act as a DNA-binding transcriptional repressor. Here, we confirm the interaction of RhoH and KAISO in murine lymphoma cells. The significant enrichment of KAISO binding at the *Bcl-6* promoter by ChIP-qPCR shown here and decreased expression of *Bcl-6* in *KOTg* lymphoma cells after RhoH re-expression strongly suggest that KAISO is a transcriptional repressor of *Bcl-6* in this model, which is consistent with previous data published about the role of KAISO in normal GC B cells [20]. Additional studies in human lymphoma cells interrogating RhoH and KAISO expression would be informative, particularly as splenomegaly and increased GC cell proliferation due to increased *Bcl-6* and *c-Myc* expression has been noted in the absence of *Kaiso* in mice [20].

BLIMP-1, a gene whose expression is required for terminal differentiation to plasma cells, is a direct target of BCL-6 [35,36]. Significantly lower *BLIMP-1* mRNA expression levels have been found in 26% of an aggressive type of DLBCL harbouring BCL-6 translocations [36]. shRNA-mediated knockdown of *BCL-6* expression in the *BCL-6*-translocated RCK8 and OCI-Ly8 human DLBCL cell lines led to up-regulation of BLIMP-1 mRNA and protein [23]. Consistent with these previous studies, our data show that the reduced expression of BLIMP-1 is associated with increased BCL-6 expression in *KOTg* lymphoma cells, and re-expression of RhoH leads to both repressed BCL-6 expression and increased BLIMP-1 expression. Thus, our data support the hypothesis that deregulated BCL-6 expression is responsible for suppressing BLIMP-1 expression and provide additional evidence for a role of BLIMP-1 in mediating a more aggressive lymphoma phenotype.

Overall, it appears that dysregulated expression of RhoH alters the function or expression of multiple genes involved in B cell apoptosis and proliferation. Our findings suggest a previously unrecognized role of RhoH in the development of *Bcl-6*-driven lymphoma via the interaction with KAISO, highlight a role of KAISO in transcriptional silencing of *Bcl-6*, and suggest that KAISO may function as a tumour suppressor in lymphoma. Since RhoH function may be regulated at the transcriptional level by its unique ITAM-like motif [6] or by

values, n = 3. All of the Western blots were performed three times, and representative figures of those blots are shown. Data show mean ± SD, * $p < 0.05$; ** $p < 0.01$; *** $p < 0.001$; ns: no significant difference (f) Subcellular localization of KAISO detected by immunofluorescence staining in a *KOTg* lymphoma cell line transduced with empty vector (Control) or HA-RhoH (RhoH). Immunofluorescence shows staining with anti-KAISO antibody (red) and nuclear staining with Hoechst33342 (blue). The arrows denote individual cells stained with KAISO. Scale bars are 5 μm. The images were captured by Leica TCS SP8 (STED One) at 100X magnification.

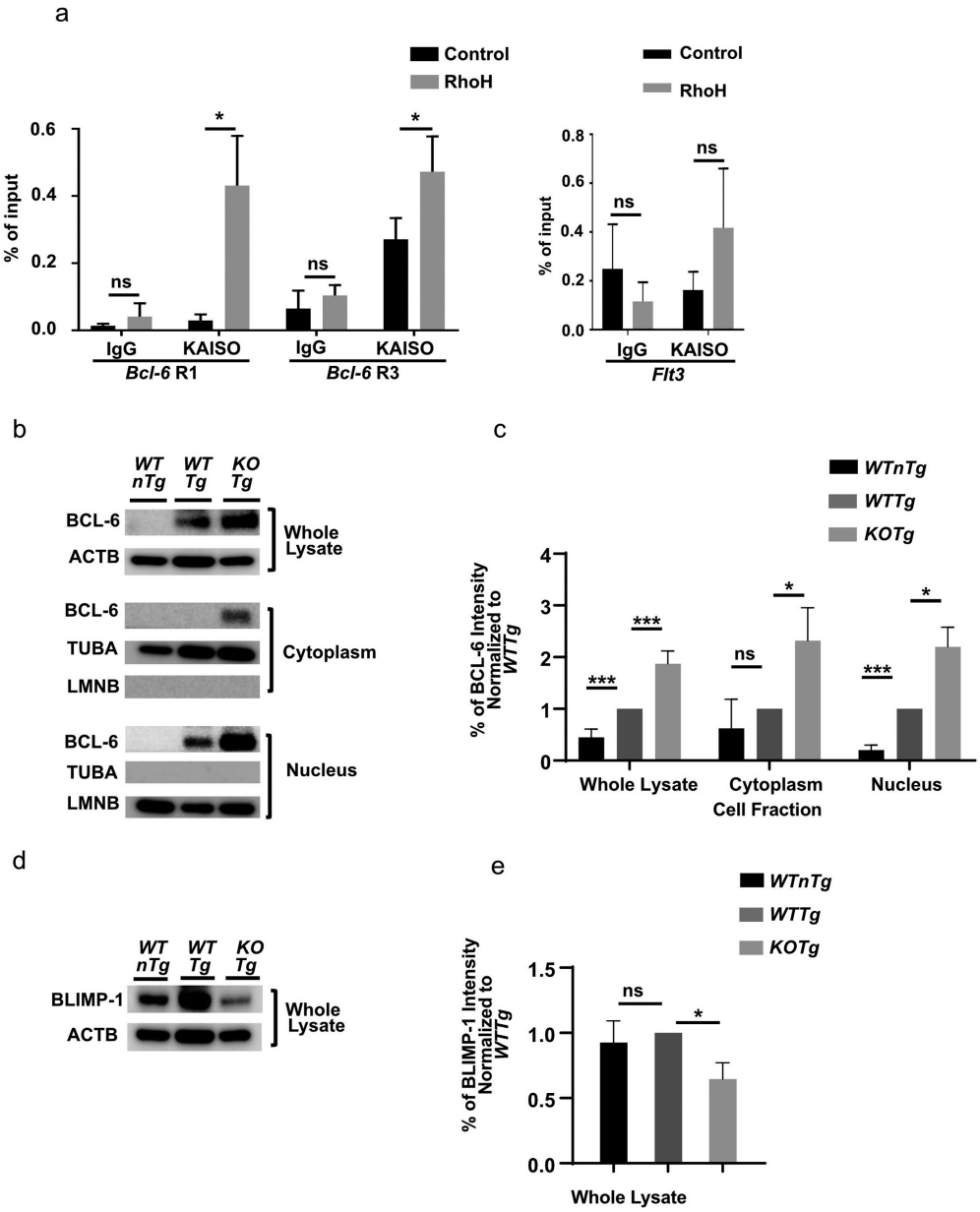

Figure 4. KAISO binds to the *Bcl-6* promoter, and deletion of *Rhoh* leads to de-repression of the KAISO target *Bcl-6* and the downregulation of the BCL-6 target *Blimp-1*. (a) Chromatin Immunoprecipitation (ChIP) was performed in a *KOTg* lymphoma cell line transduced with empty vector (Control) or HA-RhoH (RhoH) against anti-KAISO antibody or IgG control followed by qPCR with primers specific for known KAISO binding sites at the *Bcl-6* promoter, including the two regulatory regions R1 (bp, −900~-450) and R3 (bp, +2165~+2423). The Flt3 gene promoter was selected as a negative control. n = 3; data show mean ± SD, * $p < 0.05$; ns: no significant difference. (b) BCL-6 expression by Western blot analysis in the whole cell lysates (top panel), cytoplasmic (middle panel), and nuclear (lower panel) fractions of sorted $CD19^+$ spleen cells harvested from *WTnTg, WTTg*, and *KOTg* mice. (c) Intensity of BCL-6 Western blot bands by Image J analysis in the whole cell lysates, cytoplasmic, and nuclear fractions of sorted $CD19^+$ spleen cells harvested from *WTnTg, WTTg*, and *KOTg* mice. BCL-6 band intensity is normalized to the internal control, and those values are normalized to the *WTTg* BCL-6 internal control normalized values, n = 4 for the whole lysates and n = 3 for the cytoplasmic and nuclear fractions. (d) BLIMP-1 expression by Western blot analysis in whole cell lysates of sorted $CD19^+$ spleen cells isolated from *WTnTg, WTTg*, and *KOTg* mice shown. (e) Intensity of BLIMP-1 Western blot bands by Image J analysis in the whole cell lysates of sorted $CD19^+$ spleen cells harvested from *WTnTg, WTTg*, and *KOTg* mice. BLIMP-1 band intensity is normalized to the internal control, and those values are normalized to the *WTTg* BLIMP-1 internal control normalized values, n = 4. α-TUBULIN (TUBA) and LAMIN B1 (LMNB) were used as loading controls for cytoplasmic and nuclear fractions, respectively, and β-Actin (ACTB) was used as a loading control for whole cell lysates. All of the Western blots were performed four times for the whole cell lysates and three times for the cytoplasmic and nuclear fractions. Representative figures of those blots are shown. Data show mean ± SD, * $p < 0.05$; *** $p < 0.001$; ns: no significant difference.

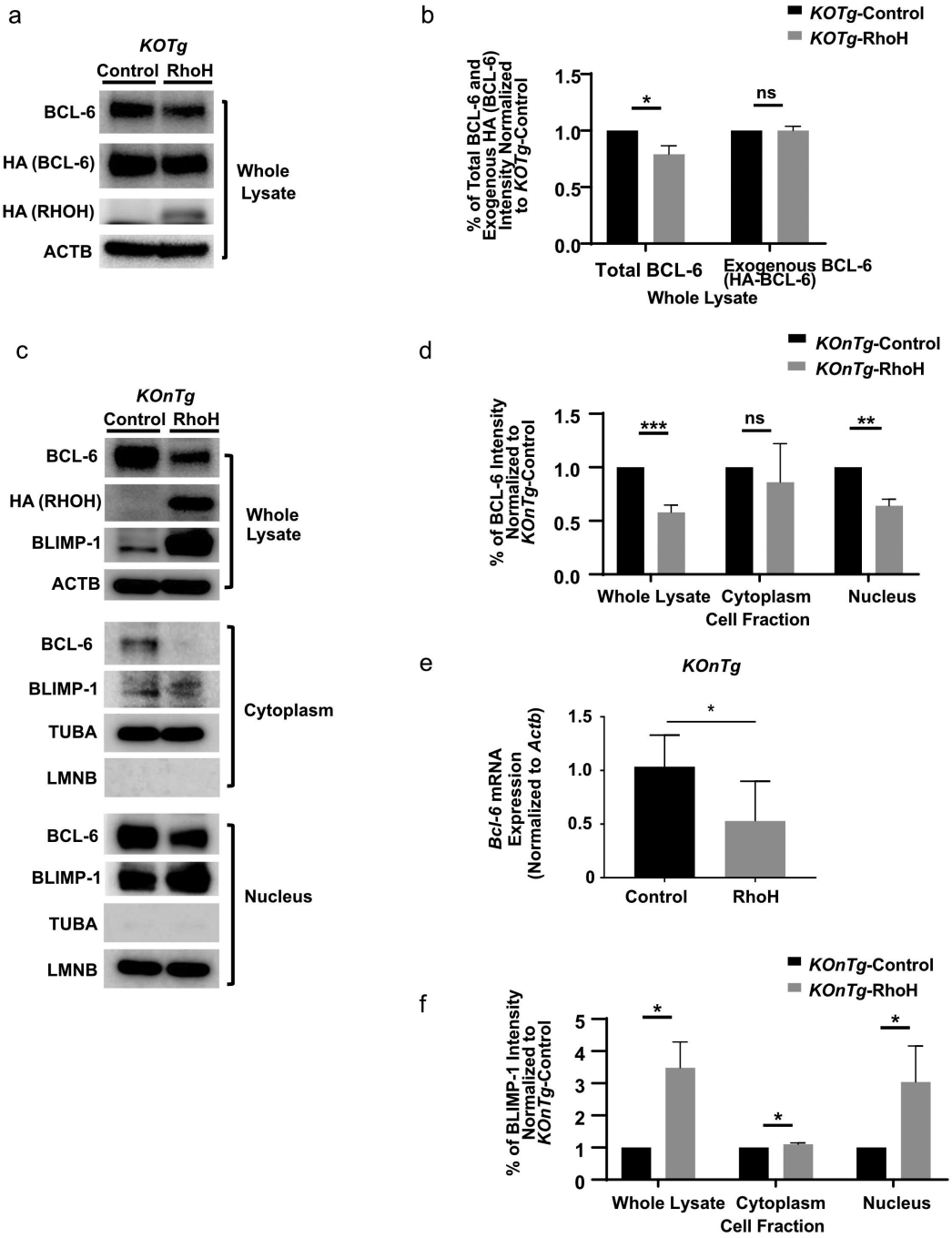

Figure 5. RhoH re-expression in lymphoma cells reverses alterations of BCL-6 and BLIMP-1 expression. (a) Western blot analysis showing the expression of BCL-6, HA tagged BCL-6, or HA tagged RhoH in the whole cell lysates of a *KOTg* lymphoma cell line transduced with empty vector (Control) or HA tagged RhoH (RhoH). (b) Intensity of total BCL-6 (BCL-6) and exogenous BCL-6 (HA tagged BCL-6) Western blot bands by Image J analysis in the whole cell lysates of a *KOTg* lymphoma cell line transduced with empty vector (Control) or HA tagged RhoH (RhoH). BCL-6 and HA tagged BCL-6 band intensity is normalized to the internal control, and those values are normalized to the *KOTg*-Control BCL-6 or HA tagged BCL-6 internal control normalized values, respectively, n = 3. (c) Western blot analysis showing the expression of BCL-6, HA tagged RhoH, and BLIMP-1 in the whole cell lysates (top panel), cytoplasmic (middle panel), and nuclear (lower panel) fractions of a *KOnTg* B cell line transduced with empty vector (Control) or HA tagged RhoH (RhoH). (d) Intensity of BCL-6 Western blot bands by Image J analysis in the whole cell lysates, cytoplasmic, and nuclear fractions of a *KOnTg* B cell line transduced with empty vector (Control) or HA tagged RhoH (RhoH). BCL-6 band intensity is normalized to the internal control, and those values are normalized to the *KOnTg*-Control BCL-6 internal control normalized values, n = 3. (e) *Bcl-6* mRNA expression by qPCR in a *KOnTg* B cell line transduced with empty vector (Control) or RhoH (RhoH) (right panel). β-Actin (*Actb*) was used as an internal control, n = 6; mean ± SD, * $p < 0.05$.) (f) Intensity of BLIMP-1 Western blot bands by Image J analysis in the whole cell lysates, cytoplasmic, and nuclear fractions of a *KOnTg* B cell malignant cell line transduced with empty vector (Control) or HA tagged RhoH (RhoH). BLIMP-1 band intensity is normalized to the internal control, and those values are

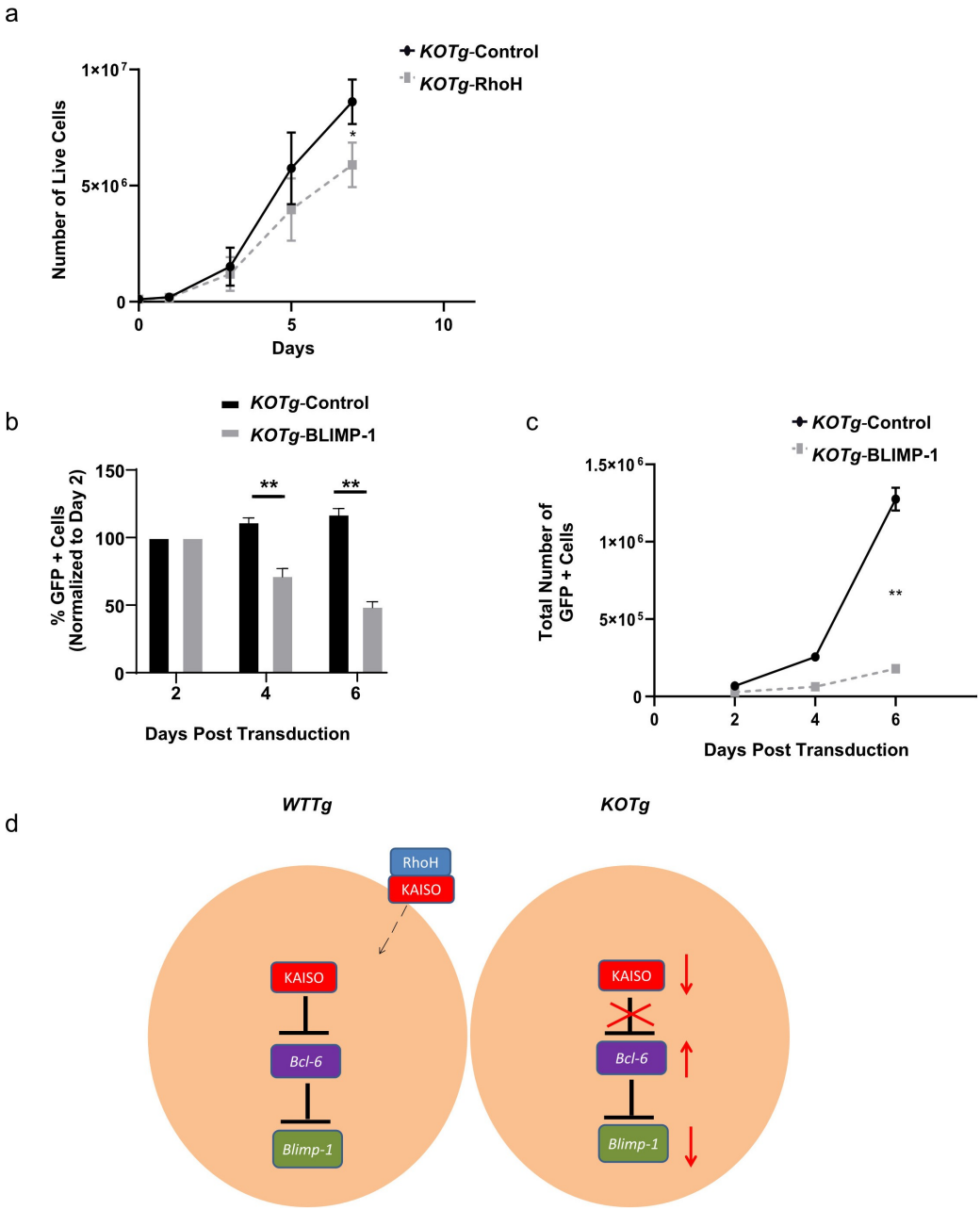

Figure 6. Re-expression of RhoH in *KO* lymphoma cells leads to decreased proliferation. (a) *In vitro* growth of a *KOTg* lymphoma cell line transduced with a RhoH-expressing retrovirus vector (*KOTg*-RhoH) *versus* empty vector (*KOTg*-Control), n = 4. (b) *In vitro* growth of a *KOTg* lymphoma cell line transduced with a BLIMP-1-expressing retrovirus vector with GFP (*KOTg*-BLIMP-1) *versus* empty vector with GFP (*KOTg*-Control). Flow cytometry was used to identify the GFP^+ cell populations. The percentage of GFP^+ cells on Days 4 and 6 were normalized to the percentage of GFP^+ cells detected two days post transduction, n = 3. (c) *In vitro* growth of a *KOTg* lymphoma cell line transduced with a BLIMP-1-expressing retrovirus vector with GFP (*KOTg*-BLIMP-1) *versus* empty vector with GFP (*KOTg*-Control), n = 3. Flow cytometry was used to identify the GFP^+ cell populations. Data show mean ± SD. * $p < 0.05$, ** $p < 0.001$. (d) Working model for RhoH involvement in tumour cell proliferation. In *WTTg* cells without RhoH deficiency, RhoH interacts with KAISO, and KAISO is present in the nucleus where it represses the transcription of *Bcl-6*. Transcription factor BCL-6 represses the *Blimp-1* gene, which codes for the BLIMP-1 transcription factor important in the terminal differentiation of B cells into plasma cells. In *KOTg* cells with RhoH deficiency, decreased KAISO levels result in de-repression of *Bcl-6*. BCL-6 expression increases, which is followed by decreased BLIMP-1 expression.

normalized to the *KOnTg*-Control BLIMP-1 internal control normalized values, n = 3. For (a) and (c), β-Actin (ACTB) was used as a loading control for whole cell lysates; for (c), α-TUBULIN (TUBA) and LAMIN B1 (LMNB) were additionally used as loading controls for cytoplasmic and nuclear fractions, respectively. All of the Western blots were performed three times, and representative figures of those blots are shown. Data show mean ± SD, * $p < 0.05$; ** $p < 0.01$; *** $p < 0.001$; ns: no significant difference.

lysosomal degradation [37] via chaperone-mediated autophagy, further studies will determine whether modulation of RhoH interaction with KAISO could represent a novel therapeutic approach in B cell malignancies.

Acknowledgments

We appreciate Dr. Laura Pasqualucci for providing us the *Iμ-HABcl-6* transgenic mouse model and Dr. Scott Armstrong for helpful discussions. We thank the IDDRC Cellular Imaging Core for immunofluorescence imaging and image processing. We thank Karen Arias, Maria Suarez, Mursal Hassan, Timothy Colby, and Teresa Ortiz for assistance in manuscript formatting and submission.

Disclosure statement

No potential conflict of interest was reported by the author(s).

Funding

This work was supported by National Institutes of Health grants CA202756, P50CA206963, and CA113969 (to D.A. W.), R01 CA196703 (to R.C), and P50 HD105351 (to the IDDRC Cellular Imaging Core).

ORCID

Felicia Ciuculescu http://orcid.org/0000-0001-9630-7055

References

[1] Hodge RG, Ridley AJ. Regulating Rho GTPases and their regulators. Nat Rev Mol Cell Biol. 2016;17:496–510.
[2] Dallery E, Galiegue-Zouitina S, Collyn-d'Hooghe M, et al. TTF, a gene encoding a novel small G protein, fuses to the lymphoma- associated LAZ3 gene by t(3;4) chromosomal translocation. Oncogene. 1995;10:2171–2178.
[3] Preudhomme C, Roumier C, Hildebrand MP, et al. Nonrandom 4p13 rearrangements of the RhoH/TTF gene, encoding a GTP- binding protein, in non-Hodgkin's lymphoma and multiple myeloma. Oncogene. 2000;19:2023–2032.
[4] Pasqualucci L, Neumeister P, Goossens T, et al. Hypermutation of multiple proto-oncogenes in B-cell diffuse large-cell lymphomas. Nature. 2001;412:341–346.
[5] Troeger A, Williams DA. Hematopoietic-specific Rho GTPases Rac2 and RhoH and human blood disorders. Exp Cell Res. 2013;319:2375–2383.
[6] Gu Y, Chae H, Siefring J, et al. RhoH, a GTPase recruits and activates Zap70 required for T cell receptor signaling and thymocyte development. Nat Immunol. 2006;7:1182–1190.
[7] Chae HD, Lee KE, Williams DA, et al. Cross-talk between RhoH and Rac1 in regulation of actin cytoskeleton and chemotaxis of hematopoietic progenitor cells. Blood. 2008;111:2597–2605.
[8] Iwasaki T, Katsumi A, Kiyoi H, et al. Prognostic implication and biological roles of RhoH in acute myeloid leukaemia. Eur J Haematol. 2008;81:454–460.
[9] Sanchez-Aguilera A, Rattmann I, Drew DZ, et al. Involvement of RhoH GTPase in the development of B-cell chronic lymphocytic leukemia. Leukemia. 2010;24:97–104.
[10] Gundogdu MS, Liu H, Metzdorf D, et al. The haematopoietic GTPase RhoH modulates IL3 signalling through regulation of STAT activity and IL3 receptor expression. Mol Cancer. 2010;9:225.
[11] Troeger A, Johnson AJ, Wood J, et al. RhoH is critical for cell-microenvironment interactions in chronic lymphocytic leukemia in mice and humans. Blood. 2012;119:4708–4718.
[12] Fueller F, Kubatzky KF. The small GTPase RhoH is an atypical regulator of haematopoietic cells. Cell Commun Signal. 2008;6:6.
[13] Hiraga J, Katsumi A, Iwasaki T, et al. Prognostic analysis of aberrant somatic hypermutation of RhoH gene in diffuse large B cell lymphoma. Leukemia. 2007;21:1846–1847.
[14] Zhang B, Zhang Y, Shacter E. Rac1 inhibits apoptosis in human lymphoma cells by stimulating Bad phosphorylation on Ser-75. Mol Cell Biol. 2004;24:6205–6214.
[15] Gu Y, Jasti AC, Jansen M, et al. RhoH, a hematopoietic-specific Rho GTPase, regulates proliferation, survival, migration, and engraftment of hematopoietic progenitor cells. Blood. 2005;105:1467–1475.
[16] Krivtsov AV, Feng Z, Lemieux ME, et al. H3K79 methylation profiles define murine and human MLL-AF4 leukemias. Cancer Cell. 2008;14:355–368.
[17] Cattoretti G, Pasqualucci L, Ballon G, et al. Deregulated BCL6 expression recapitulates the pathogenesis of human diffuse large B cell lymphomas in mice. Cancer Cell. 2005;7:445–455.
[18] Hans CP, Weisenburger DD, Greiner TC, et al. Confirmation of the molecular classification of diffuse large B-cell lymphoma by immunohistochemistry using a tissue microarray. Blood. 2004;103:275–282.
[19] Mino A, Troeger A, Brendel C, et al. RhoH participates in a multi-protein complex with the zinc finger protein kaiso that regulates both cytoskeletal structures and chemokine-induced T cells. Small GTPases. 2018;9:260–273.
[20] Koh DI, Yoon JH, Kim MK, et al. Kaiso is a key regulator of spleen germinal center formation by repressing Bcl6 expression in splenocytes. Biochem Biophys Res Commun. 2013;442:177–182.
[21] Shaffer AL, Yu X, He Y, et al. BCL-6 represses genes that function in lymphocyte differentiation, inflammation, and cell cycle control. Immunity. 2000;13:199–212.
[22] Fearon DT, Manders P, Wagner SD. Arrested differentiation, the self-renewing memory lymphocyte, and vaccination. Science. 2001;293:248–250.
[23] Mandelbaum J, Bhagat G, Tang H, et al. BLIMP1 is a tumor suppressor gene frequently disrupted in activated B cell-like diffuse large B cell lymphoma. Cancer Cell. 2010;18:568–579.
[24] Crequer A, Troeger A, Patin E, et al. Human RHOH deficiency causes T cell defects and susceptibility to EV-HPV infections. J Clin Invest. 2012;122:3239–3247.

[25] Chai N, Chang HE, Nicolas E, et al. Assembly of hepatitis B virus envelope proteins onto a lentivirus pseudotype that infects primary human hepatocytes. J Virol. 2007;81:10897–10904.
[26] Galiegue-Zouitina S, Delestre L, Dupont C, et al. Underexpression of RhoH in Hairy Cell Leukemia. Cancer Res. 2008;68:4531–4540.
[27] Prokhortchouk A, Hendrich B, Jorgensen H, et al. The p120 catenin partner Kaiso is a DNA methylation-dependent transcriptional repressor. Genes Dev. 2001;15:1613–1618.
[28] Yoon HG, Chan DW, Reynolds AB, et al. N-CoR mediates DNA methylation-dependent repression through a methyl CpG binding protein Kaiso. Mol Cell. 2003;12:723–734.
[29] Daniel JM, Spring CM, Crawford HC, et al. The p120 (ctn)-binding partner Kaiso is a bi-modal DNA-binding protein that recognizes both a sequence-specific consensus and methylated CpG dinucleotides. Nucleic Acids Res. 2002;30:2911–2919.
[30] Daniel JM, Ireton RC, Reynolds AB. Monoclonal antibodies to Kaiso: a novel transcription factor and p120ctn-binding protein. Hybridoma. 2001;20:159–166.
[31] Daniel JM, Reynolds AB. The catenin p120(ctn) interacts with Kaiso, a novel BTB/POZ domain zinc finger transcription factor. Mol Cell Biol. 1999;19:3614–3623.
[32] Koh DI, Han D, Ryu H, et al. KAISO, a critical regulator of p53-mediated transcription of CDKN1A and apoptotic genes. Proc Natl Acad Sci U S A. 2014;111:15078–15083.
[33] Koh DI, An H, Kim MY, et al. Transcriptional activation of APAF1 by KAISO (ZBTB33) and p53 is attenuated by RelA/p65. Biochim Biophys Acta. 2015;1849:1170–1178.
[34] Blattler A, Farnham PJ. Cross-talk between site-specific transcription factors and DNA methylation states. J Biol Chem. 2013;288:34287–34294.
[35] Reljic R, Wagner SD, Peakman LJ, et al. Suppression of signal transducer and activator of transcription 3-dependent B lymphocyte terminal differentiation by BCL-6. J Exp Med. 2000;192:1841–1848.
[36] Tunyaplin C, Shaffer AL, Angelin-Duclos CD, et al. Direct repression of prdm1 by Bcl-6 inhibits plasmacytic differentiation. J Immunol. 2004;173:1158–1165.
[37] Troeger A, Chae HD, Senturk M, et al. A unique carboxyl-terminal insert domain in the hematopoietic-specific, GTPase-deficient Rho GTPase RhoH regulates post-translational processing. J Biol Chem. 2013;288:36451–36462.